
Time Series Deconfounder: Estimating Treatment Effects over Time in the Presence of Hidden Confounders

Ioana Bica^{1,2} Ahmed M. Alaa³ Mihaela van der Schaar^{2,3,4}

Abstract

The estimation of treatment effects is a pervasive problem in medicine. Existing methods for estimating treatment effects from longitudinal observational data assume that there are no hidden confounders. This assumption is not testable in practice and, if it does not hold, leads to biased estimates. In this paper, we develop the Time Series Deconfounder, a method that leverages the assignment of multiple treatments over time to enable the estimation of treatment effects even in the presence of hidden confounders. The Time Series Deconfounder uses a novel recurrent neural network architecture with multitask output to build a factor model over time and infer substitute confounders that render the assigned treatments conditionally independent. Then it performs causal inference using the substitute confounders. We provide a theoretical analysis for obtaining unbiased causal effects of time-varying exposures using the Time Series Deconfounder. Using simulations we show the effectiveness of our method in deconfounding the estimation of treatment responses in longitudinal data.

1. Introduction

Forecasting the patient’s response to treatments assigned over time represents a crucial problem in the medical domain. The increasing availability of observational data from electronic health records makes it possible to learn individualized treatment responses from longitudinal disease trajectories containing information about patient covariates and treatments assignments over time (Robins, 1986; Robins et al., 2000; Robins & Hernán, 2008; Soleimani et al., 2017; Schulam & Saria, 2017; Lim et al., 2018). However, existing

methods assume that all confounders — variables affecting both the treatment assignment and the potential outcomes — are observed, an assumption which is not testable in practice¹ and probably not true in many circumstances.

To understand why the presence of hidden confounders introduces bias, consider the problem of estimating treatment effects for patients diagnosed with cancer. They are often prescribed multiple treatments at the same time, including chemotherapy, radiotherapy and/or immunotherapy based on the characteristics of their tumour. These treatments are adjusted if the tumour size decreases or increases. Moreover, the treatment strategy is also changed as the patient starts to develop drug resistance (Vlachostergios & Faltas, 2018) or the toxicity levels of the drugs increase (Kroschinsky et al., 2017). Drug resistance and toxicity levels are multi-cause confounders since they affect not only the multiple causes (treatments), but also the outcome for the patient (e.g. mortality, risk factors). However, drug resistance and toxicity may not be observed and, even if observed, may not be recorded in the electronic health record. Estimating, for example, the effect of chemotherapy on the cancer progression in the patient without accounting for the dependence on drug resistance and toxicity levels will produce biased results. This is why, in the presence of hidden confounders, existing methods are prone to fail in identifying the true causal effects of time-varying exposures.

(Wang & Blei, 2018) developed theory for deconfounding — adjusting for the bias introduced by the existence of hidden confounders in observational data — in the *static* causal inference setting and noted that the existence of multiple causes makes this task easier. In particular, (Wang & Blei, 2018) observed that the dependencies in the assignment of multiple causes in the static setting can be used to infer latent variables that render the causes conditionally independent and act as substitutes for the hidden confounders.

In this paper, we propose the Time Series Deconfounder, a method that enables the unbiased estimation of treatment responses *over time* in the presence of hidden confounders, by taking advantage of the potential sequential assignment of multiple treatments. We draw from the main idea in

¹Department of Engineering Science, University of Oxford, Oxford, United Kingdom ²The Alan Turing Institute, London, United Kingdom ³Department of Electrical Engineering, UCLA, Los Angeles, USA ⁴University of Cambridge, Cambridge, United Kingdom. Correspondence to: Ioana Bica <ioana.bica@eng.ox.ac.uk>.

¹Since counterfactuals are never observed, it is not possible to test for the existence of hidden confounders that could affect them.

(Wang & Blei, 2018), but note that the estimation of the hidden confounders in the longitudinal setting is significantly more complex than in the static setting, not just because the hidden confounders may vary over time but in particular because the hidden confounders may be affected by previous treatment assignments and covariates. In this case, standard latent variable models are no longer applicable, as they cannot capture these time dependencies.

The Time Series Deconfounder relies on building a factor model *over time* to obtain substitutes for the hidden confounder which, together with the observed variables render the assigned causes conditionally independent. Through theoretical analysis we show how the substitute confounders can be used to satisfy the identifiability conditions in the potential outcomes framework for time-varying exposures (Robins & Hernán, 2008) and obtain unbiased estimates of individualized treatment responses, using weaker assumptions than standard methods. Following our theory, we propose a novel deep learning architecture, based on a recurrent neural network with multi-task output and variational dropout in order to build such a factor model over time and infer substitutes for the hidden confounders in practice.

The Time Series Deconfounder shifts the need for observing all confounders (untestable condition) to being able to construct a good factor model over time (testable condition). To assess how well the factor model captures the distribution of assigned causes, we extend the use of predictive checks (Rubin, 1984; Wang & Blei, 2018) over time and compute p -values at each timestep. We perform experiments on a simulated dataset where we can control the amount of hidden confounding applied and a state-of-the-art pharmacokinetic-pharmacodynamic (PK-PD) model of tumour growth (Geng et al., 2017) and show how the Time Series Deconfounder allows us to deconfound the estimation of treatment responses in longitudinal data. To the best of our knowledge, this represents the first method for learning hidden confounders in the time series setting.

2. Related Work

Most of the previous methods for performing causal inference have focused on the static setting (Hill, 2011; Wager & Athey, 2017; Alaa & van der Schaar, 2017; Yoon et al., 2018), and less attention has been given to the time series setting. We discuss methods developed for estimating treatment effects over time, as well as methods for inferring substitute hidden confounders in the static setting.

Potential outcomes for time-varying treatment assignments. Standard methods for performing counterfactual inference in longitudinal data are found in the epidemiology literature and include the g -computation formula, g -estimation of structural nested mean models and inverse

probability of weighting estimation of marginal structural models (Robins, 1986; 1994; Robins et al., 2000; Robins & Hernán, 2008). Additionally, (Lim et al., 2018) improves on the standard marginal structural models by using recurrent neural networks to estimate the propensity weights and treatment response. While these methods have been widely used in forecasting treatment responses, they are all based on the assumption that there are no hidden confounders in the observational data. Our paper proposes a method for deconfounding such outcome models, by inferring substitutes for the hidden confounders which can lead to unbiased estimates of the potential outcomes.

The potential outcomes framework has also been extended to the continuous time setting by (Lok et al., 2008). Several methods using Bayesian nonparametrics have been proposed for estimating the treatment responses in continuous time (Xu et al., 2016; Soleimani et al., 2017; Schulam & Saria, 2017), again assuming that there are no hidden confounders. However, in this paper, we focus on deconfounding the estimation of treatment responses in the discrete time setting.

Latent variable models for estimating hidden confounders. The most similar work to ours is (Wang & Blei, 2018), who proposed the deconfounder, an algorithm that infers latent variables that act as substitutes for the hidden confounders and then performs causal inference in the static multi-cause setting. The deconfounder involves finding a good factor model of the assigned causes which can be used to estimate the substitute confounder. Then, the deconfounder fits an outcome model for estimating the causal effects using the inferred latent variables. Our paper extends the theory for the deconfounder to the time-varying treatment assignment setting and shows how the inferred latent variables can lead to sequential strong ignorability. To estimate the substitute confounders, (Wang & Blei, 2018) used standard factor models (Tipping & Bishop, 1999; Ranganath et al., 2015), which are only applicable in the static setting. To build a factor model in the longitudinal setting, we propose a novel recurrent neural network architecture with multitask output and variational dropout.

Several other methods have been proposed for taking advantage of the multiplicity of assigned causes in the static setting and capture shared latent confounding (Tran & Blei, 2017; Heckerman, 2018; Ranganath & Perotte, 2018). However, these works are based on Pearl’s causal framework (Pearl, 2009) and use structural equation models, while our method deconfounds the estimation of treatment effects in the potential outcomes framework (Neyman, 1923; Rubin, 1978; Robins & Hernán, 2008). Alternative methods for dealing with hidden confounders in the static setting involve using proxy variables as noisy substitutes for latent confounders (Lash et al., 2014; Kuroki & Pearl, 2014; Louizos et al., 2017; Lee et al., 2018).

3. Problem Formulation

At hospital visit (timestep) t , let the random variables $\mathbf{X}_t^{(i)} \in \mathcal{X}_t$ be the time-dependent covariates for patient (i) and $\mathbf{A}_t^{(i)} = [A_{t1}^{(i)} \dots A_{tk}^{(i)}] \in \mathcal{A}_t$ be the possible assignment of k treatments (causes). Treatments can be either binary and/or continuous. Static features about the patient, such as genetic information do not change our theory and, for simplicity, we assume they are included in the observed covariates. We want to estimate the effect of the treatments assigned until timestep $T^{(i)}$ on an outcome of interest $\mathbf{Y}^{(i)} \in \mathcal{Y}$ that would be observed at timestep $T^{(i)} + 1$.

Observational data about the patient consists of realizations of the previously described random variables: $\mathcal{D}^{(i)} = \{\mathbf{x}_t^{(i)}, \mathbf{a}_t^{(i)}\}_{t=1}^{T^{(i)}} \cup \{\mathbf{y}_{T^{(i)}+1}^{(i)}\}$, with samples collected at discrete and regular timesteps. Electronic health records consist of data for N independent patients. For simplicity, we omit the patient superscript (i) unless it is explicitly needed.

Let $\bar{\mathbf{A}}_t = (\mathbf{A}_1, \dots, \mathbf{A}_t) \in \bar{\mathcal{A}}_t$ be the history of treatments and let $\bar{\mathbf{X}}_t = (\bar{\mathbf{X}}_1, \dots, \bar{\mathbf{X}}_t) \in \bar{\mathcal{X}}_t$ be the history of covariates until timestep t . Let $\bar{\mathbf{A}} = \bar{\mathbf{A}}_T$ and $\bar{\mathbf{X}} = \bar{\mathbf{X}}_T$ be the entire treatment and covariate history respectively, with $\bar{\mathbf{A}} \in \bar{\mathcal{A}} = \bar{\mathcal{A}}_T$ and $\bar{\mathbf{X}} \in \bar{\mathcal{X}} = \bar{\mathcal{X}}_T$ and let $\bar{\mathbf{a}} \in \bar{\mathcal{A}}$ and $\bar{\mathbf{x}} \in \bar{\mathcal{X}}$ be realisations of these random variables.

We adopt the potential outcomes framework proposed by (Rubin, 1978) and (Neyman, 1923), and extended by (Robins & Hernán, 2008) to take into account time-varying treatments in order to estimate the causal effect of $\bar{\mathbf{A}}$ on \mathbf{Y} . Let $\mathbf{Y}(\bar{\mathbf{a}})$ be the potential outcome, either factual or counterfactual, for the treatment history $\bar{\mathbf{a}}$. For each patient, we estimate the individualized treatment effect over time:

$$\mathbb{E}[\mathbf{Y}(\bar{\mathbf{a}}) \mid \bar{\mathbf{X}}], \quad (1)$$

for each possible treatment assignments $\bar{\mathbf{a}} \in \bar{\mathcal{A}}$.

The observational data can be used to obtain $\mathbb{E}[\mathbf{Y} \mid \bar{\mathbf{A}} = \bar{\mathbf{a}}, \bar{\mathbf{X}}]$. Under certain assumptions, also known as identifiability conditions, these estimates are unbiased so that $\mathbb{E}[\mathbf{Y}(\bar{\mathbf{a}}) \mid \bar{\mathbf{X}}] = \mathbb{E}[\mathbf{Y} \mid \bar{\mathbf{A}} = \bar{\mathbf{a}}, \bar{\mathbf{X}}]$. These conditions include Assumptions 1 and 2, which are standard among the existing methods and can be tested in practice.

Assumption 1: Consistency. If $\bar{\mathbf{A}} = \bar{\mathbf{a}}$ for a given patient, then $\mathbf{Y}(\bar{\mathbf{a}}) = \mathbf{Y}$ for that patient.

Assumption 2: Positivity (Overlap) (Imai & Van Dyk, 2004): If $P(\bar{\mathbf{A}}_{t-1} = \bar{\mathbf{a}}_{t-1}, \bar{\mathbf{X}}_t = \bar{\mathbf{x}}_t) \neq 0$ then $P(\bar{\mathbf{A}}_t = \bar{\mathbf{a}}_t \mid \bar{\mathbf{A}}_{t-1} = \bar{\mathbf{a}}_{t-1}, \bar{\mathbf{X}}_t = \bar{\mathbf{x}}_t) > 0$ for all $\bar{\mathbf{a}}_t$.

In addition to these two assumptions, existing methods also assume *sequential strong ignorability*:

$$\mathbf{Y}(\bar{\mathbf{a}}) \perp\!\!\!\perp \mathbf{A}_t \mid \bar{\mathbf{A}}_{t-1}, \bar{\mathbf{X}}_t, \quad (2)$$

for all $\bar{\mathbf{a}} \in \bar{\mathcal{A}}$ and for all $t = 1, \dots, T$. This condition holds if there are no hidden confounders, an assumption which is

untestable in practice. To understand why this is the case, note that the sequential strong ignorability assumption requires the conditional independence of the treatments with all of the potential outcomes, both factual and counterfactual. Since the counterfactuals are never observed, it is not possible to test for this conditional independence.

In this paper, we assume that there are hidden confounders. Consequently, using standard methods for computing $\mathbb{E}[\mathbf{Y}(\bar{\mathbf{a}}) \mid \bar{\mathbf{A}}, \bar{\mathbf{X}}]$ from the dataset will result in biased estimates since the hidden confounders introduce a dependence between the treatments at each timestep and the potential outcomes ($\mathbf{Y}(\bar{\mathbf{a}}) \not\perp\!\!\!\perp \mathbf{A}_t \mid \bar{\mathbf{A}}_{t-1}, \bar{\mathbf{X}}_t$) and therefore:

$$\mathbb{E}[\mathbf{Y}(\bar{\mathbf{a}}) \mid \bar{\mathbf{X}}] \neq \mathbb{E}[\mathbf{Y} \mid \bar{\mathbf{A}} = \bar{\mathbf{a}}, \bar{\mathbf{X}}]. \quad (3)$$

By extending the method proposed by (Wang & Blei, 2018) for deconfounding causal inference in the static setting, we take advantage of the multiple treatment assignments at each timestep to infer a sequence of latent variables $\bar{\mathbf{Z}} = (\mathbf{Z}_1, \dots, \mathbf{Z}_T) \in \bar{\mathcal{Z}}$ that can be used as substitutes for the unobserved confounders. We will then show how $\bar{\mathbf{Z}}$ can be used to identify the estimation of potential outcomes.

4. Time Series Deconfounder

The idea behind the Time Series Deconfounder is that multi-cause confounders introduce dependencies between the treatments. As treatment assignments change over time we infer substitutes for the hidden confounders that take advantage of patient history to capture these dependencies.

4.1. Factor Model

The Time Series Deconfounder builds a factor model to capture the distribution of the causes over time. At timestep t , the factor model constructs the latent variable $\mathbf{z}_t = g(\bar{\mathbf{h}}_{t-1})$, where $\bar{\mathbf{h}}_{t-1} = (\bar{\mathbf{a}}_{t-1}, \bar{\mathbf{x}}_{t-1}, \bar{\mathbf{z}}_{t-1})$ is the realisation of the history $\bar{\mathbf{H}}_{t-1}$. Along with the observed covariates, \mathbf{z}_t renders the assigned causes conditionally independent:

$$p(a_{t1}, \dots, a_{tk} \mid \mathbf{z}_t, \mathbf{x}_t) = \prod_{j=1}^k p(a_{tj} \mid \mathbf{z}_t, \mathbf{x}_t). \quad (4)$$

Figure 1(a) illustrates the corresponding graphical model for timestep t . The assignment of the causes is modelled through parameters $\theta_{1:k}$. The factor model of the assigned causes is a latent variable model with joint distribution:

$$p(\theta_{1:k}, \bar{\mathbf{x}}, \bar{\mathbf{z}}, \bar{\mathbf{a}}) = p(\theta_{1:k})p(\bar{\mathbf{x}}) \cdot \prod_{t=1}^T \left(p(\mathbf{z}_t \mid \bar{\mathbf{h}}_{t-1}) \prod_{j=1}^k p(a_{tj}^{(i)} \mid \mathbf{z}_t, \mathbf{x}_t, \theta_j) \right). \quad (5)$$

The distribution of assigned causes $p(\bar{\mathbf{a}})$ is the corresponding marginal.

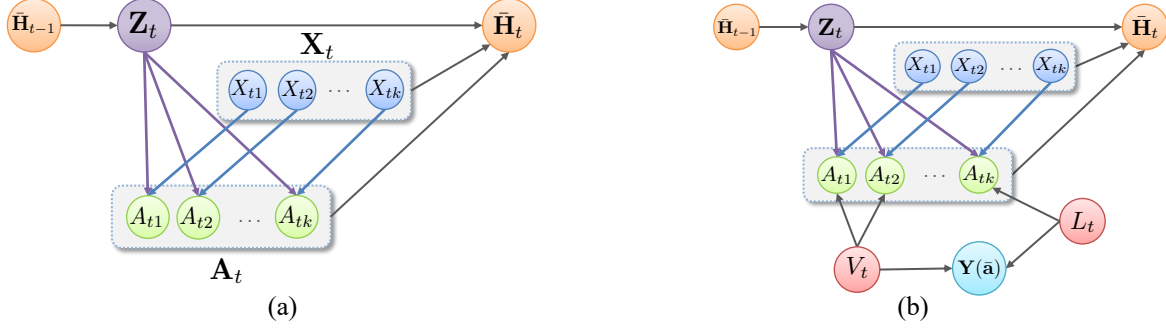


Figure 1. (a) Graphical model for the factor model. At timestep t , the latent variable \mathbf{Z}_t is built as a function of the history: $\mathbf{Z}_t = g(\bar{\mathbf{H}}_{t-1})$ such that, together with \mathbf{X}_t , it renders the assigned causes conditionally independent: $p(a_{t1}, \dots, a_{tk} | \mathbf{z}_t, \mathbf{x}_t) = \prod_{j=1}^k p(a_{tj} | \mathbf{z}_t, \mathbf{x}_t)$. The variables can be connected to the potential outcomes $\mathbf{Y}(\bar{\mathbf{a}})$ in any way. (b) Graphical model explanation for why the factor model construction ensures that \mathbf{Z}_t captures all of the multi-cause hidden confounders.

By taking advantage of the dependencies between the multiple treatment assignments, the factor model allows us to infer the sequence of latent variables $\bar{\mathbf{Z}}$ that render the assigned causes conditionally independent. Through this factor model construction, we can rule out the existence of other multi-cause confounders which are not captured by \mathbf{Z}_t . Consider the graphical model in Figure 1(b). By contradiction, assume that there exists another multi-cause confounder V_t not captured by \mathbf{Z}_t . Then, by d -separation the conditional independence between the assigned causes given \mathbf{Z}_t and \mathbf{X}_t does not hold any more. This argument cannot be used for single-cause confounders, such as L_t , which are only affecting one of the causes and the potential outcomes. Thus, we make the sequential single strong ignorability assumption (no hidden single cause confounders).

Assumption 3: Sequential single strong ignorability.

$$\mathbf{Y}(\bar{\mathbf{a}}) \perp\!\!\!\perp A_{tj} | \mathbf{X}_t, \bar{\mathbf{H}}_{t-1}, \quad (6)$$

$$\forall \bar{\mathbf{a}} \in \bar{\mathcal{A}}, \forall t \in \{0, \dots, T\} \text{ and } \forall j \in \{1, \dots, k\}.$$

Causal inference relies on assumptions. Existing methods for estimating treatment effects over time assume that there are no multi-cause and single-cause hidden confounders. In this paper, we make the *weaker* assumption that there are no single-cause hidden confounders. While this assumption is also untestable in practice, as the number of causes increases for each timestep, it becomes increasingly weaker: the more causes we observe, the less likely it becomes for a hidden confounder to affect only one of them.

Theorem 1: If the distribution of the assigned causes $p(\bar{\mathbf{a}})$ can be written as the factor model $p(\theta_{1:k}, \bar{\mathbf{x}}, \bar{\mathbf{z}}, \bar{\mathbf{a}})$ then we obtain *sequential ignorable treatment assignment*:

$$\mathbf{Y}(\bar{\mathbf{a}}) \perp\!\!\!\perp (A_{t1}, \dots, A_{tk}) | \bar{\mathbf{A}}_{t-1}, \bar{\mathbf{X}}_t, \bar{\mathbf{Z}}_t, \quad (7)$$

for all $\bar{\mathbf{a}} \in \bar{\mathcal{A}}$ and for all $t \in \{0, \dots, T\}$. Proof in Appendix.

Theorem 1 is proved by leveraging the sequential single strong ignorability assumption, the fact that the sub-

stitute confounders \mathbf{Z}_t are inferred without any knowledge of the potential outcomes $\mathbf{Y}(\bar{\mathbf{a}})$ and the fact that the causes (A_{t1}, \dots, A_{tk}) are jointly independent given \mathbf{Z}_t and \mathbf{X}_t . The result means that, at each timestep, the variables $\bar{\mathbf{X}}_t, \bar{\mathbf{Z}}_t, \bar{\mathbf{A}}_{t-1}$ contain all of the dependencies between the potential outcomes and the assigned causes $\bar{\mathbf{A}}_t$ and therefore, can be used to estimate the causal effects of $\bar{\mathbf{A}}_t$.

4.2. Outcome Model

The Time Series Deconfounder then fits an existing outcome model (Robins et al., 2000; Robins & Hernán, 2008), to compute $\mathbb{E}[\mathbf{Y} | \bar{\mathbf{A}} = \bar{\mathbf{a}}, \bar{\mathbf{X}}, \bar{\mathbf{Z}}]$, where $\bar{\mathbf{Z}}$ is estimated from the factor model. After adding \mathbf{Z}_t to the data, Theorem 1 tells us that sequential strong ignorability now holds. Adding this result to assumptions 1 and 2, the identifiability conditions in the potential outcomes framework are now satisfied. Therefore, unbiased estimates of the individualised treatment effects can be obtained from observational data:

$$\mathbb{E}[\mathbf{Y}(\bar{\mathbf{a}}) | \bar{\mathbf{X}}, \bar{\mathbf{Z}}] = \mathbb{E}[\mathbf{Y} | \bar{\mathbf{A}} = \bar{\mathbf{a}}, \bar{\mathbf{X}}, \bar{\mathbf{Z}}]. \quad (8)$$

4.3. Predictive Checks over Time

The theory holds if the fitted factor model captures well the distribution of the assigned causes. This condition can be assessed by extending predictive model checking (Rubin, 1984) to the time-series setting. We compute p -values over time to evaluate how similar the distribution of the treatments, as learnt by the factor model, is with the distribution of the treatments in a held-out (validation) set of patients.

At each timestep t , for the patients in the validation set, we obtain M replicas of their treatment assignments $\{\mathbf{a}_{t,\text{rep}}^{(i)}\}_{i=1}^M$ by sampling from the factor model. The replicated treatment assignments are compared with the actual treatment assignments, $\mathbf{a}_{t,\text{val}}$, using the test statistic $T(\mathbf{a}_t)$:

$$T(\mathbf{a}_t) = \mathbb{E}_{\mathbf{Z}}[\log p(\mathbf{a}_t | \mathbf{Z}_t, \mathbf{X}_t)], \quad (9)$$

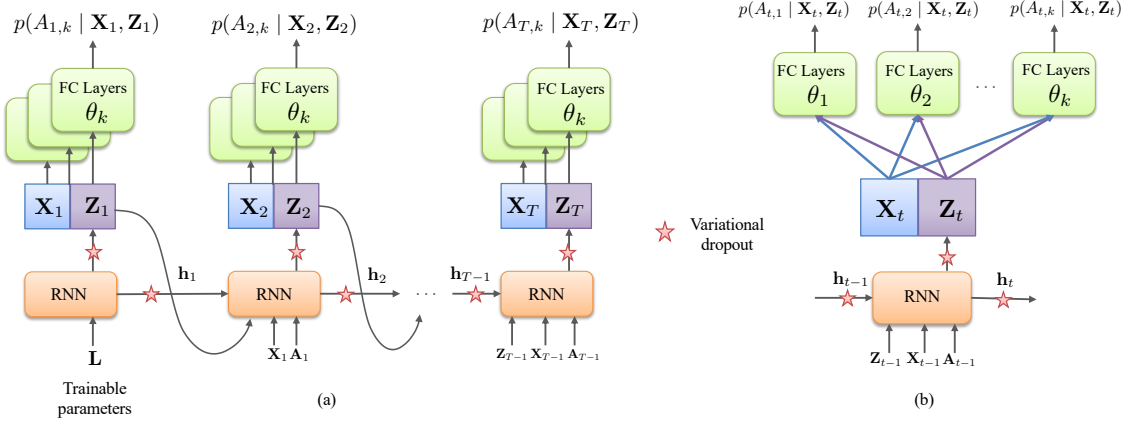


Figure 2. (a) Proposed factor model implementation. The latent variables \mathbf{Z}_t are generated by a recurrent neural network as a function of the history $\bar{\mathbf{H}}_{t-1}$, obtained through the RNN hidden state \mathbf{h}_t and the current input. Multitask output is used to construct the treatments such that they are conditionally independent given \mathbf{Z}_t and \mathbf{X}_t . (b) Closer look at a single timestep in the factor model over time.

related to the marginal log likelihood (Wang & Blei, 2018). The predictive p -value for timestep t is computed as follows:

$$\frac{1}{M} \sum_{i=1}^M \mathbf{1} \left(T \left(\mathbf{a}_{t,\text{rep}}^{(i)} \right) < T \left(\mathbf{a}_{t,\text{val}} \right) \right), \quad (10)$$

where $\mathbf{1}(\cdot)$ represents the indicator function.

If the model captures well the distribution of the assigned causes, then the test statistics for the treatment replicas are similar to the test statistic for the treatments in the validation set, which makes 0.5 the ideal p -value in this case.

5. Factor Model over Time in Practice

Due to the fact that we are dealing with time-varying treatment assignments, we cannot use standard factor models, such as Principal Component Analysis (Tipping & Bishop, 1999) or Deep Exponential Families (Ranganath et al., 2015), as they can only be applied in the static setting. Using the theory developed for the factor model over time we introduce a practical implementation based on a recurrent neural network (RNN) with multitask output and variational dropout as illustrated in Figure 2.

The recurrent part of the architecture is used for inferring the substitute confounders such that they depend on the history:

$$\mathbf{Z}_1 = \text{RNN}(\mathbf{L}), \quad (11)$$

$$\mathbf{Z}_t = \text{RNN}(\bar{\mathbf{Z}}_{t-1}, \bar{\mathbf{X}}_{t-1}, \bar{\mathbf{A}}_{t-1}, \mathbf{L}). \quad (12)$$

where \mathbf{L} consists of parameters initialized randomly and trained with the rest of the parameters in the RNN. Note that the size of the RNN output is D_Z and this specifies the size of the substitutes confounder. In our experiments, we use a Long Short Term Memory unit (Hochreiter & Schmidhuber, 1997) as the RNN in the factor model.

Moreover, to infer the assigned causes at timestep t , $\mathbf{A}_t = [A_{t,1}, \dots, A_{t,k}]$ such that they are conditionally independent given the latent variable \mathbf{Z}_t and the observed covariates \mathbf{X}_t , we propose using multitask multilayer perceptrons (MLP) consisting of fully connected (FC) layers:

$$A_{t,j} = \text{FC}(\mathbf{X}_t, \mathbf{Z}_t; \theta_j) \quad (13)$$

for all $j = 1, \dots, k$ and for all $t = 1, \dots, T$, where θ_j are the parameters in the FC layers used to obtain $A_{t,j}$. In our experiments, we use a single FC hidden layer before the output layer. For binary treatments, the sigmoid activation function is used in the output layer. For continuous treatments, MC dropout (Gal & Ghahramani, 2016a) can instead be applied in the FC layers to obtain $p(A_{t,j} | \mathbf{X}_t, \mathbf{Z}_t)$.

To model the probabilistic nature of factor models we incorporate variational dropout (Gal & Ghahramani, 2016b) in the RNN as illustrated in Figure 2. The application of variational dropout enables us to obtain samples from \mathbf{Z}_t and from the treatment assignments $A_{t,j}$. These samples also allow us to obtain treatment replicas and to compute predictive checks over time.

Using the treatment assignments from the observational dataset, the factor model can be trained using gradient descent based methods. We note that the proposed factor model architecture follows from the theory developed in Section 4 where at each timestep the latent variable \mathbf{Z}_t is built as a function of the history (parametrised by an RNN). Additionally, the multitask output is essential for modelling the conditional independence between the assigned treatments given the latent confounder generated by the RNN and the observed covariates.

The use of neural networks to implement the factor model enables us to model complex relationships between the covariates, hidden confounders and treatment assignments.

This makes the proposed factor model suitable for medical application where complex diseases are involved.

6. Experiments on Synthetic Data

In real-world datasets ground truth information about the hidden confounders is not available. Thus, we propose evaluating the Time Series Deconfounder on synthetic data where we can vary the effect of hidden confounding.

6.1. Simulated Dataset

To keep the data simulation process as general as possible, we propose using p -order autoregressive processes. We build a dataset consisting of single-cause observed covariates, multi-cause time-varying hidden confounders, treatment assignments and outcomes.

We simulate k time-varying covariates representing single cause confounders as follows:

$$X_{t,j} = \frac{1}{p} \left(\sum_{i=1}^p \alpha_{i,j} X_{t-i,j} + \sum_{i=1}^p \omega_{i,k} A_{t-i,j} \right) + \eta_t, \quad (14)$$

for $j = 1, \dots, k$ and $\alpha_{i,k} \sim \mathcal{N}(0, 0.5^2)$, $\omega_{i,k} \sim \mathcal{N}(1 - (i/p), (1/p)^2)$ and $\eta_t \sim \mathcal{N}(0, 0.01^2)$.

The multi-cause hidden confounder is generated as follows:

$$Z_t = \frac{1}{p} \left(\sum_{i=1}^p \beta_i Z_{t-i} + \sum_{i=1}^p \left(\sum_{j=1}^k \lambda_{i,j} A_{t-i,j} \right) \right) + \epsilon_t \quad (15)$$

where $\epsilon_t \sim \mathcal{N}(0, 1)$, $\lambda_{i,j} \sim \mathcal{N}(0, 0.5^2)$, $\beta_i \sim \mathcal{N}(1 - (i/p), (1/p)^2)$. The value of the hidden confounder changes over time and is affected by the treatment assignment.

The assignment of each treatment A_{tj} will depend on the covariate X_{tj} (single-cause confounder) and hidden confounded Z_t (multi-cause confounder).

$$\pi_{tj} = \gamma_A \hat{Z}_t + (1 - \gamma_A) \hat{X}_{tj} \quad (16)$$

$$A_{tj} | \pi_{tj} \sim \text{Bernoulli}(\sigma(\lambda \pi_{tj})), \quad (17)$$

where \hat{X}_{tj} and \hat{Z}_t are the sum of the covariates and confounders respectively over the last p timesteps, $\lambda = 15$, $\sigma(\cdot)$ is the sigmoid function and γ_A controls the amount of hidden confounding applied to the treatment assignments.

The outcome is also obtained as a function of the covariates and hidden confounder:

$$\mathbf{Y}_{t+1} = \gamma_Y Z_{t+1} + (1 - \gamma_Y) \left(\frac{1}{k} \sum_{j=1}^k X_{t+1,j} \right) \quad (18)$$

where γ_Y controls the amount of hidden confounding applied to the outcome. Note that in this case, we repeat

the outcome problem, as formulated in Section 3 for each timestep in the sequence.

Each experiment simulated a dataset consisting of 5000 patients, with trajectories between 20 and 30 timesteps, and $k = 3$ covariates and treatments. To induce time dependencies we set $p = 5$. Each dataset undergoes a 80/10/10 split for training, validation and testing respectively. Hyperparameter optimisation is performed for each factor model trained to estimate the hidden confounders as explained in the Appendix B. The results in the following sections are averaged across 30 different simulated datasets.

6.2. Evaluating Factor Model using Predictive Checks

The underlying theory behind being able to use the substitute confounders to obtain unbiased treatment responses relies on the fact that the factor model captures well the distribution of the assigned causes. To assess the suitability of our proposed factor model architecture, we compare it with the following two baselines: RNN without multitask output (predicting the k treatment assignments by passing \mathbf{X}_t and \mathbf{Z}_t through a hidden layer and having an output layer with k neurons) and multilayer perceptron (MLP) used instead of the RNN at each timestep for generating \mathbf{Z}_t . The MLP factor model does not use the entire history for generating \mathbf{Z}_t . The implementation and hyperparameter optimisation details for these baselines can be found in Appendix C.

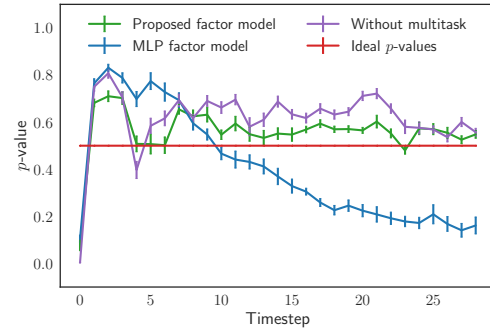


Figure 3. Predictive checks over time. The figure shows the average p -values at each timestep and the standard error in the results.

Figure 3 shows the p -values over time computed for the test set in 30 simulated datasets with $\gamma_A = \gamma_Y = 0.5$. The p -values for the MLP factor model decrease over time, which means that there is a consistent distribution mismatch between the treatment assignments learnt by this model and the ones in the test set. Conversely, the predictive checks for our proposed factor model are closer to the ideal p -value of 0.5. This illustrates the fact that having an architecture capable of capturing time-dependencies and accumulating information from the past for inferring the latent confounders is

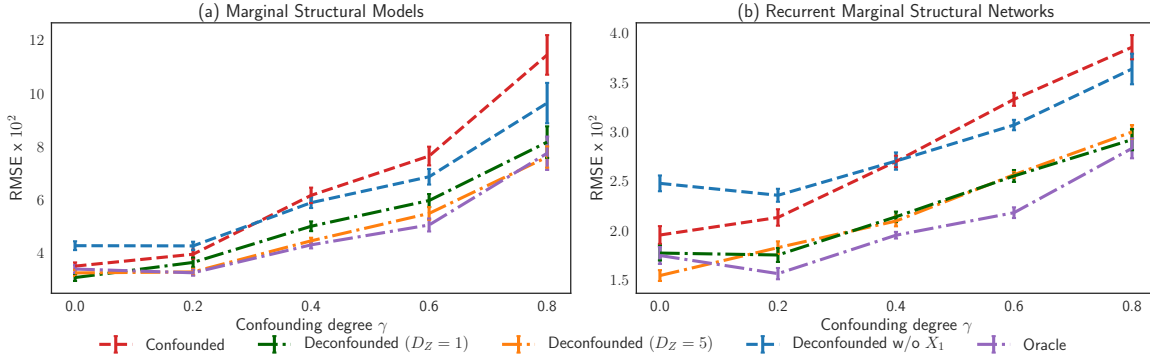


Figure 4. Results for deconfounding one-step ahead predictions of treatment responses in two outcome models: (a) Marginal Structural Models (MSM) and (b) Recurrent Marginal Structural Networks (R-MSN). The average RMSE and the standard error in the results are computed for 30 dataset simulations for each different degree of confounding, as measured by γ .

crucial. Moreover, the performance for the RNN without multitask is similar to our proposed model, which indicates that the imposed factor model constraint does not affect the performance in capturing the distribution of the causes.

6.3. Benchmark Outcome Models

We evaluate how well the Time Series Deconfounder can remove bias from the estimation of treatment responses when used in conjunction with the following outcome models:

Standard Marginal Structural Models (MSMs). MSMs (Robins et al., 2000; Hernán et al., 2001) have been widely used in epidemiology to perform causal inference in longitudinal data. MSMs compute propensity weights using logistic/linear regression to construct a pseudo-population from the observational data that resembles the one in a clinical trial. This removes selection bias and the bias introduced by time-dependent confounders. The implementation of this outcome model is similar to the one in (Hernán et al., 2001; Howe et al., 2012). Full details in Appendix D.1.

Recurrent Marginal Structural Networks (R-MSNs). R-MSNs (Lim et al., 2018) also apply propensity weighting to adjust for time-dependent confounders, but they estimate the propensity scores using RNNs instead. The use of RNNs is more robust to changes in the treatment assignment policy. For details on how the model was implemented and optimised see Appendix D.2.

6.4. Deconfounding the Estimation of Treatment Responses over Time

In our dataset simulations, the parameters γ_A and γ_Y control the amount of hidden confounding applied to the treatment assignments and outcomes respectively. We vary the amount of hidden confounding applied through $\gamma_A = \gamma_Y = \gamma$. The benchmark outcome models are then trained without infor-

mation about \bar{Z} (confounded), with the simulated \bar{Z} (oracle), as well as after applying the Time Series Deconfounder with different model specifications. To highlight the importance of the sequential single strong ignorability assumption, we also apply the Time Series Deconfounder after removing X_1 from the dataset, thus violating the assumption.

Figure 4 illustrates the root mean squared error (RMSE) obtained for one-step ahead prediction of treatment responses in this experimental set-up. The results indicate that the Time Series Deconfounder gives unbiased estimates of the treatment responses, i.e. close to the estimates obtained using the simulated (oracle) confounders. The method is also robust to model misspecification, performing similarly both when $D_Z = 1$ (simulated dimensionality of hidden confounders) and when $D_Z = 5$ (misspecified dimensionality for the inferred confounders). Even in the case when there are no hidden confounders ($\gamma = 0$), using the additional information from \bar{Z} does not harm the estimations.

When the sequential single strong ignorability assumption is invalidated, namely when the latent variables \bar{Z} are inferred after removing the single cause confounder X_1 from the dataset, we obtain biased estimates of the treatment responses. The performance in this case, however, is comparable to the performance when there is no control for the hidden confounders.

Source of gain: To understand the source of gain in the Time Series Deconfounder, consider why the outcome models fail in the scenarios when there are hidden confounders. MSMs and R-MSNs make the implicit assumption that the treatment assignments depend only on the observed history. The existence of any multi-cause confounders not captured by the history results in biased estimates of both the propensity weights and of the outcomes. On the other hand, the construction in our factor model rules out the existence of any multi-cause confounders which are not captured by Z_t .

By augmenting the data available to the outcome models with the substitute confounders, we eliminate these biases.

6.5. Identifying Trends of the Hidden Confounders

Since the simulated hidden confounders in our datasets vary over time, we can assess how well the factor model has identified their trends. Figure 5 shows the cross-correlation between the simulated (oracle) confounders and the predicted confounders as well as a specific example of how the trends in the simulated hidden confounder for a patient in the test set are identified by our factor model. Both results are illustrated from a dataset simulated with $\gamma = 0.4$.

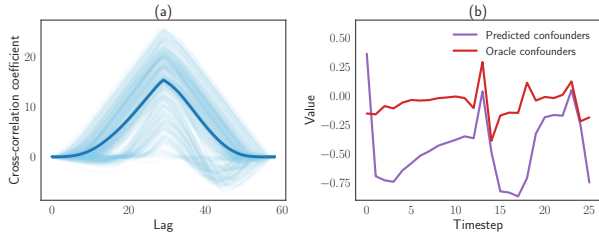


Figure 5. (a) Cross-correlation between predicted hidden confounder and simulated hidden confounder. (b) Example of how the trends in the simulated hidden confounder are identified.

7. Model of Tumour Growth

To show the applicability of our method in a realistic medical set-up, we use the state-of-the-art pharmacokinetic-pharmacodynamic (PK-PD) model of tumour growth proposed by (Geng et al., 2017) and used by (Lim et al., 2018). The PK-PD model characterizes patients suffering from lung cancer and models the evolution of their tumour under the combined effects of chemotherapy and radiotherapy.

The volume of tumour after t days since diagnosis is modelled as follows:

$$V(t) = \left(\underbrace{1 + \rho \log\left(\frac{K}{V(t-1)}\right)}_{\text{Tumor growth}} - \underbrace{\beta_c C(t)}_{\text{Chemotherapy}} - \underbrace{(\alpha_r d(t) + \beta_r d(t)^2)}_{\text{Radiotherapy}} + \underbrace{e_t}_{\text{Noise}} \right) V(t-1) \quad (19)$$

where the parameters $K, \rho, \beta_c, \alpha_r, \beta_r$ are sampled from the prior distributions described in (Geng et al., 2017) and $e_t \sim \mathcal{N}(0, 0.01^2)$. $C(t)$ is the concentration of the chemotherapy drugs and $d(t)$ represents the dose of radiation. The chemotherapy and radiotherapy prescriptions are modelled as Bernoulli random variables which directly depend on the size of the tumour. For full details about how the drug prescriptions and dosages are modelled refer to

(Geng et al., 2017; Lim et al., 2018).

To account for heterogeneity among patient responses, due to, for example genetic features (Bartsch et al., 2007), the prior means for β_c and α_r are adjusted according to the three patient subgroups as described in (Lim et al., 2018). The patient subgroup $S^{(i)} \in \{1, 2, 3\}$ represents a confounder because it affects the growth of the tumour and subsequently the assignment of treatments. We reproduced the experimental set-up in (Lim et al., 2018) and simulated datasets consisting of 10000 patients for training, 1000 for validation and 1000 for testing with trajectory of up to 60 timesteps. We simulated 30 datasets and averaged the results for testing the MSM and R-MSN outcome models without the information about patient types (confounded), with the true simulated patient types (oracle), as well as after applying the Time Series Deconfounder with $D_Z \in \{1, 5, 10\}$.

Table 1. Average RMSE $\times 10^2$ (normalised by the maximum tumour volume) and the standard error in the results for predicting the effect of chemotherapy and radiotherapy on the tumour volume.

Outcome model	MSM	R-MSN
Confounded	7.29 ± 0.14	5.31 ± 0.16
Deconfounded ($D_Z = 1$)	6.47 ± 0.16	4.76 ± 0.17
Deconfounded ($D_Z = 5$)	6.25 ± 0.14	4.79 ± 0.19
Deconfounded ($D_Z = 10$)	6.31 ± 0.11	4.54 ± 0.17
Oracle	6.92 ± 0.19	5.00 ± 0.15

The results in Table 1 indicate that our method can also infer substitutes for static hidden confounders such as patient subgroups which affect the treatment responses over time.

8. Conclusion

The availability of observational data consisting of longitudinal information about patients prompted the development of many methods for modelling the effects of treatments on the disease progression in patients. All existing methods make the untestable assumption that there are no hidden confounders. In the longitudinal setting, this assumption is even more problematical than in the static setting. As the state of the patient changes over time and the complexity of the treatment assignments and responses increases, it becomes much easier to miss important confounding information.

In this paper, we developed the Time Series Deconfounder, a method that takes advantage of the patterns in the multiple treatment assignments over time to infer latent variables that can be used as substitutes for the hidden confounders. Moreover, we proposed a novel deep learning architecture based on a recurrent neural network with multitask output and variational dropout that can be used to build a factor model over time and compute the substitute confounders in practice. The Time Series Deconfounder enables the

unbiased estimation of treatments responses in longitudinal data in the presence of multi-cause hidden confounders.

Acknowledgements

The research presented in this paper was supported by The Alan Turing Institute and the US Office of Naval Research (ONR).

References

- Abadi, M., Agarwal, A., Barham, P., Brevdo, E., Chen, Z., Citro, C., Corrado, G. S., Davis, A., Dean, J., Devin, M., Ghemawat, S., Goodfellow, I., Harp, A., Irving, G., Isard, M., Jia, Y., Jozefowicz, R., Kaiser, L., Kudlur, M., Levenberg, J., Mané, D., Monga, R., Moore, S., Murray, D., Olah, C., Schuster, M., Shlens, J., Steiner, B., Sutskever, I., Talwar, K., Tucker, P., Vanhoucke, V., Vasudevan, V., Viégas, F., Vinyals, O., Warden, P., Wattenberg, M., Wicke, M., Yu, Y., and Zheng, X. TensorFlow: Large-scale machine learning on heterogeneous systems, 2015. URL <https://www.tensorflow.org/>. Software available from tensorflow.org.
- Alaa, A. M. and van der Schaar, M. Bayesian inference of individualized treatment effects using multi-task gaussian processes. In *Advances in Neural Information Processing Systems*, pp. 3424–3432, 2017.
- Bartsch, H., Dally, H., Popanda, O., Risch, A., and Schmezer, P. Genetic risk profiles for cancer susceptibility and therapy response. In *Cancer Prevention*, pp. 19–36. Springer, 2007.
- Gal, Y. and Ghahramani, Z. Dropout as a bayesian approximation: Representing model uncertainty in deep learning. In *international conference on machine learning*, pp. 1050–1059, 2016a.
- Gal, Y. and Ghahramani, Z. A theoretically grounded application of dropout in recurrent neural networks. In *Advances in neural information processing systems*, pp. 1019–1027, 2016b.
- Geng, C., Paganetti, H., and Grassberger, C. Prediction of treatment response for combined chemo-and radiation therapy for non-small cell lung cancer patients using a bio-mathematical model. *Scientific reports*, 7(1):13542, 2017.
- Heckerman, D. Accounting for hidden common causes when inferring cause and effect from observational data. *arXiv preprint arXiv:1801.00727*, 2018.
- Hernán, M. A., Brumback, B., and Robins, J. M. Marginal structural models to estimate the joint causal effect of nonrandomized treatments. *Journal of the American Statistical Association*, 96(454):440–448, 2001.
- Hill, J. L. Bayesian nonparametric modeling for causal inference. *Journal of Computational and Graphical Statistics*, 20(1):217–240, 2011.
- Hochreiter, S. and Schmidhuber, J. Long short-term memory. *Neural computation*, 9(8):1735–1780, 1997.
- Howe, C. J., Cole, S. R., Mehta, S. H., and Kirk, G. D. Estimating the effects of multiple time-varying exposures using joint marginal structural models: alcohol consumption, injection drug use, and hiv acquisition. *Epidemiology (Cambridge, Mass.)*, 23(4):574, 2012.
- Imai, K. and Van Dyk, D. A. Causal inference with general treatment regimes: Generalizing the propensity score. *Journal of the American Statistical Association*, 99(467): 854–866, 2004.
- Kallenberg, O. *Foundations of modern probability*. Springer Science & Business Media, 2006.
- Kroschinsky, F., Stölzel, F., von Bonin, S., Beutel, G., Kochanek, M., Kiehl, M., and Schellongowski, P. New drugs, new toxicities: severe side effects of modern targeted and immunotherapy of cancer and their management. *Critical Care*, 21(1):89, 2017.
- Kuroki, M. and Pearl, J. Measurement bias and effect restoration in causal inference. *Biometrika*, 101(2):423–437, 2014.
- Lash, T. L., Fox, M. P., MacLehose, R. F., Maldonado, G., McCandless, L. C., and Greenland, S. Good practices for quantitative bias analysis. *International journal of epidemiology*, 43(6):1969–1985, 2014.
- Lee, C., Mastronarde, N., and van der Schaar, M. Estimation of individual treatment effect in latent confounder models via adversarial learning. *arXiv preprint arXiv:1811.08943*, 2018.
- Lim, B., Alaa, A., and van der Schaar, M. Forecasting treatment responses over time using recurrent marginal structural networks. In *Advances in Neural Information Processing Systems*, pp. 7493–7503, 2018.
- Lok, J. J. et al. Statistical modeling of causal effects in continuous time. *The Annals of Statistics*, 36(3):1464–1507, 2008.
- Louizos, C., Shalit, U., Mooij, J. M., Sontag, D., Zemel, R., and Welling, M. Causal effect inference with deep latent-variable models. In *Advances in Neural Information Processing Systems*, pp. 6446–6456, 2017.

- Neyman, J. Sur les applications de la théorie des probabilités aux expériences agricoles: Essai des principes. *Roczniki Nauk Rolniczych*, 10:1–51, 1923.
- Pearl, J. *Causality*. Cambridge university press, 2009.
- Platt, R. W., Schisterman, E. F., and Cole, S. R. Time-modified confounding. *American journal of epidemiology*, 170(6):687–694, 2009.
- Ranganath, R. and Perotte, A. Multiple causal inference with latent confounding. *arXiv preprint arXiv:1805.08273*, 2018.
- Ranganath, R., Tang, L., Charlin, L., and Blei, D. Deep exponential families. In *Artificial Intelligence and Statistics*, pp. 762–771, 2015.
- Robins, J. A new approach to causal inference in mortality studies with a sustained exposure period—application to control of the healthy worker survivor effect. *Mathematical modelling*, 7(9-12):1393–1512, 1986.
- Robins, J. M. Correcting for non-compliance in randomized trials using structural nested mean models. *Communications in Statistics-Theory and methods*, 23(8):2379–2412, 1994.
- Robins, J. M. and Hernán, M. A. Estimation of the causal effects of time-varying exposures. In *Longitudinal data analysis*, pp. 547–593. Chapman and Hall/CRC, 2008.
- Robins, J. M., Hernan, M. A., and Brumback, B. Marginal structural models and causal inference in epidemiology, 2000.
- Rubin, D. B. Bayesian inference for causal effects: The role of randomization. *The Annals of statistics*, pp. 34–58, 1978.
- Rubin, D. B. Bayesianly justifiable and relevant frequency calculations for the applied statistician. *The Annals of Statistics*, pp. 1151–1172, 1984.
- Schulam, P. and Saria, S. Reliable decision support using counterfactual models. In *Advances in Neural Information Processing Systems*, pp. 1697–1708, 2017.
- Soleimani, H., Subbaswamy, A., and Saria, S. Treatment-response models for counterfactual reasoning with continuous-time, continuous-valued interventions. *arXiv preprint arXiv:1704.02038*, 2017.
- Tipping, M. E. and Bishop, C. M. Probabilistic principal component analysis. *Journal of the Royal Statistical Society: Series B (Statistical Methodology)*, 61(3):611–622, 1999.
- Tran, D. and Blei, D. M. Implicit causal models for genome-wide association studies. *arXiv preprint arXiv:1710.10742*, 2017.
- Vlachostergios, P. J. and Faltas, B. M. Treatment resistance in urothelial carcinoma: an evolutionary perspective. *Nature Reviews Clinical Oncology*, pp. 1, 2018.
- Wager, S. and Athey, S. Estimation and inference of heterogeneous treatment effects using random forests. *Journal of the American Statistical Association*, 2017.
- Wang, Y. and Blei, D. M. The blessings of multiple causes. *arXiv preprint arXiv:1805.06826*, 2018.
- Xu, Y., Xu, Y., and Saria, S. A bayesian nonparametric approach for estimating individualized treatment-response curves. In *Machine Learning for Healthcare Conference*, pp. 282–300, 2016.
- Yoon, J., Jordon, J., and van der Schaar, M. Ganite: Estimation of individualized treatment effects using generative adversarial nets. *International Conference on Learning Representations (ICLR)*, 2018.

A. Proof for Theorem 1

Before proving Theorem 1, we introduce several definitions and Lemmas that will aid with the proof. Note that these are extended from the static setting in (Wang & Blei, 2018).

Remember that at each timestep t , the random variable $\mathbf{Z}_t \in \mathcal{Z}_t$ is constructed as a function of the history until timestep t : $\mathbf{Z}_t = g(\bar{\mathbf{H}}_{t-1})$, where $\bar{\mathbf{H}}_{t-1} = (\bar{\mathbf{Z}}_{t-1}, \bar{\mathbf{X}}_{t-1}, \bar{\mathbf{A}}_{t-1})$ takes values in $\bar{\mathcal{H}}_{t-1} = \bar{\mathcal{Z}}_{t-1} \times \bar{\mathcal{X}}_{t-1} \times \bar{\mathcal{A}}_{t-1}$ and $g: \bar{\mathcal{H}}_{t-1} \rightarrow \mathcal{Z}_t$.

In order to obtain **sequential ignorable treatment assignment** using the substitutes for the hidden confounders \mathbf{Z}_t , the following property needs to hold:

$$\mathbf{Y}(\bar{\mathbf{a}}) \perp\!\!\!\perp (A_{t1}, \dots, A_{tk}) \mid \bar{\mathbf{X}}_t, \bar{\mathbf{A}}_{t-1}, \bar{\mathbf{Z}}_t, \quad (20)$$

$\forall \bar{\mathbf{a}} \in \bar{\mathcal{A}}$ and $\forall t \in \{0, \dots, T\}$.

Definition: Sequential Kallenberg construction

At timestep t , we say that the distribution of assigned causes (A_{t1}, \dots, A_{tk}) admits a sequential Kallenberg construction from random variables $\mathbf{Z}_t = g(\bar{\mathbf{H}}_{t-1})$ and \mathbf{X}_t if there exist measurable functions $f_{tj}: \mathcal{Z}_t \times \mathcal{X}_t \times [0, 1] \rightarrow \mathcal{A}_j$ and random variables $U_{jt} \in [0, 1]$, with $j = 1, \dots, k$ such that:

$$A_{tj} = f_{tj}(\mathbf{Z}_t, \mathbf{X}_t, U_{tj}), \quad (21)$$

where U_{tj} marginally follow Uniform $[0, 1]$ and jointly satisfy:

$$(U_{t1}, \dots, U_{tk}) \perp\!\!\!\perp \mathbf{Y}(\bar{\mathbf{a}}) \mid \mathbf{Z}_t, \mathbf{X}_t, \bar{\mathbf{H}}_{t-1}, \quad (22)$$

for all $\bar{\mathbf{a}} \in \bar{\mathcal{A}}$.

Lemma 1: Sequential Kallenberg construction at each timestep $t \Rightarrow$ Sequential strong ignorability. If at every timestep t , the distribution of assigned causes (A_{t1}, \dots, A_{tk}) admits a Kallenberg construction from $\mathbf{Z}_t = g(\bar{\mathbf{H}}_{t-1})$ and \mathbf{X}_t then we obtain sequential strong ignorability.

Proof for Lemma 1: Assume $\mathcal{A}_j, j = 1, \dots, m$ are Borel spaces.

For any $t \in \{1, \dots, T\}$ assume \mathcal{Z}_t and \mathcal{X}_t are measurable spaces and assume that $A_{tj} = f_{tj}(\mathbf{Z}_t, \mathbf{X}_t, U_{tj})$, where f_{tj} are measurable and

$$(U_{t1}, \dots, U_{tk}) \perp\!\!\!\perp \mathbf{Y}(\bar{\mathbf{a}}) \mid \mathbf{Z}_t, \mathbf{X}_t, \bar{\mathbf{H}}_{t-1}, \quad (23)$$

for all $\bar{\mathbf{a}} \in \bar{\mathcal{A}}$. This implies that:

$$(\mathbf{Z}_t, \mathbf{X}_t, U_{t1}, \dots, U_{tk}) \perp\!\!\!\perp \mathbf{Y}(\bar{\mathbf{a}}) \mid \mathbf{Z}_t, \mathbf{X}_t, \bar{\mathbf{H}}_{t-1}. \quad (24)$$

Since the A_{tj} 's are measurable functions of $(\mathbf{Z}_t, \mathbf{X}_t, U_{t1}, \dots, U_{tk})$ and $\bar{\mathbf{H}}_{t-1} = (\bar{\mathbf{Z}}_{t-1}, \bar{\mathbf{X}}_{t-1}, \bar{\mathbf{A}}_{t-1})$, we have that sequential strong ignorability holds:

$$(A_{t1}, \dots, A_{tk}) \perp\!\!\!\perp \mathbf{Y}(\bar{\mathbf{a}}) \mid \bar{\mathbf{X}}_t, \bar{\mathbf{A}}_{t-1}, \bar{\mathbf{Z}}_t, \quad (25)$$

$\forall \bar{\mathbf{a}} \in \bar{\mathcal{A}}$ and $\forall t \in \{0, \dots, T\}$.

Lemma 2: Factor models for the assigned causes \Rightarrow Sequential Kallenberg construction at each timestep t . Under weak regularity conditions, if the distribution of assigned causes $p(\bar{\mathbf{a}})$ can be written as the factor model $p(\theta_{1:k}, \bar{\mathbf{x}}, \bar{\mathbf{z}}, \bar{\mathbf{a}})$ then we obtain a sequential Kallenberg construction for each timestep.

Regularity condition: The domains of the causes \mathcal{A}_j for $j = 1, \dots, k$ are Borel subsets of compact intervals. Without loss of generality, assume $\mathcal{A}_j = [0, 1]$ for $j = 1, \dots, k$.

The proof for Lemma 2 uses Lemma 2.22 in (Kallenberg, 2006) (kernels and randomization): Let μ be a probability kernel from a measurable space S to a Borel space T . Then there exists some measurable function $f: S \times [0, 1] \rightarrow T$ such that if ϑ is $U(0, 1)$, then $f(s, \vartheta)$ has distribution $\mu(s, \cdot)$ for every $s \in S$.

Proof for Lemma 2: For timestep t , consider the random variables $A_{t1} \in \mathcal{A}_1, \dots, A_{tk} \in \mathcal{A}_k, \mathbf{X}_t \in \mathcal{X}_t, \mathbf{Z}_t = g(\bar{\mathbf{H}}_{t-1}) \in \mathcal{Z}_t$ and $\theta_j \in \Theta$. Assume sequential single strong ignorability holds. Without loss of generality, assume $\mathcal{A}_j = [0, 1]$ for $j = 1, \dots, k$.

From Lemma 2.22 in Kallenberg (1997), there exists some measurable function $f_{tj}: \mathcal{Z}_t \times \mathcal{X}_t \times [0, 1] \rightarrow [0, 1]$ such that $U_{tj} \sim \text{Uniform}[0, 1]$ and:

$$A_{tj} = f_{tj}(\mathbf{Z}_t, \mathbf{X}_t, U_{tj}) \quad (26)$$

and there exists some measurable function $h_{tj} : \Theta \times [0, 1] \rightarrow [0, 1]$ such that:

$$U_{tj} = h_{tj}(\theta_j, \omega_{tj}), \quad (27)$$

where $\omega_{tj} \sim \text{Uniform}[0, 1]$ and $j = 1, \dots, k$.

From our definition of the factor model we have that ω_{tj} for $j = 1, \dots, k$ are jointly independent. Otherwise, $A_{tj} = f_{tj}(\mathbf{Z}_t, \mathbf{X}_t, h_{tj}(\theta_j, \omega_{tj}))$ would not have been conditionally independent given $\mathbf{Z}_t, \mathbf{X}_t$.

Since sequential single strong ignorability holds at each timestep t , we have that $A_{tj} \perp\!\!\!\perp \mathbf{Y}(\bar{\mathbf{a}}) \mid \mathbf{X}_t, \bar{\mathbf{H}}_{t-1} \forall \bar{\mathbf{a}} \in \bar{\mathcal{A}}, \forall t \in \{0, \dots, T\}$ and for $j = 1, \dots, k$ which implies:

$$\omega_{tj} \perp\!\!\!\perp \mathbf{Y}(\bar{\mathbf{a}}) \mid \mathbf{X}_t, \bar{\mathbf{H}}_{t-1}, \quad (28)$$

$\forall \bar{\mathbf{a}} \in \bar{\mathcal{A}}$ and $\forall j \in \{1, \dots, k\}$.

Using this, we can write:

$$\begin{aligned} p(Y(\bar{\mathbf{a}}), \omega_{t1}, \dots, \omega_{tk} \mid \mathbf{X}_t, \bar{\mathbf{H}}_{t-1}) &= p(Y(\bar{\mathbf{a}}) \mid \mathbf{X}_t, \bar{\mathbf{H}}_{t-1}) \cdot p(\omega_{t1}, \dots, \omega_{tk} \mid Y(\bar{\mathbf{a}}), \mathbf{X}_t, \bar{\mathbf{H}}_{t-1}) \\ &= p(Y(\bar{\mathbf{a}}) \mid \mathbf{X}_t, \bar{\mathbf{H}}_{t-1}) \cdot \prod_{j=1}^k p(\omega_{tj} \mid \omega_{t1}, \dots, \omega_{t,j-1}, Y(\bar{\mathbf{a}}), \mathbf{X}_t, \bar{\mathbf{H}}_{t-1}) \\ &= p(Y(\bar{\mathbf{a}}) \mid \mathbf{X}_t, \bar{\mathbf{H}}_{t-1}) \cdot \prod_{j=1}^k p(\omega_{tj} \mid \mathbf{X}_t, \bar{\mathbf{H}}_{t-1}) \\ &= p(Y(\bar{\mathbf{a}}) \mid \mathbf{X}_t, \bar{\mathbf{H}}_{t-1}) \cdot p(\omega_{t1}, \dots, \omega_{tk} \mid \mathbf{X}_t, \bar{\mathbf{H}}_{t-1}) \end{aligned}$$

where the second and third steps follow from equation (28) and the fact that $\omega_{t1}, \dots, \omega_{tk}$ are jointly independent. This gives us:

$$(\omega_{t1}, \dots, \omega_{tk}) \perp\!\!\!\perp \mathbf{Y}(\bar{\mathbf{a}}) \mid \mathbf{X}_t, \bar{\mathbf{H}}_{t-1} \quad (29)$$

Moreover, since the latent random variable \mathbf{Z}_t is constructed without knowledge of $\mathbf{Y}(\bar{\mathbf{a}})$, but rather as a function of the history $\bar{\mathbf{H}}_{t-1}$ we have:

$$(\omega_{t1}, \dots, \omega_{tk}) \perp\!\!\!\perp \mathbf{Y}(\bar{\mathbf{a}}) \mid \mathbf{Z}_t, \mathbf{X}_t, \bar{\mathbf{H}}_{t-1}. \quad (30)$$

$\theta_{1:k}$ are parameters in the factor model and can be considered point masses, so we also have that:

$$(\theta_1, \dots, \theta_k) \perp\!\!\!\perp \mathbf{Y}(\bar{\mathbf{a}}) \mid \mathbf{Z}_t, \mathbf{X}_t, \bar{\mathbf{H}}_{t-1}, \quad (31)$$

Since $U_{tj} = (h_{ij}(\theta_j, \omega_{tj}))$ are measurable functions of θ_j and ω_{tj} we have that:

$$(U_{t1}, \dots, U_{tk}) \perp\!\!\!\perp \mathbf{Y}(\bar{\mathbf{a}}) \mid \mathbf{Z}_t, \mathbf{X}_t, \bar{\mathbf{H}}_{t-1} \quad (32)$$

We have thus obtained a sequential Kallenberg construction at timestep t .

Theorem 1: If the distribution of the assigned causes $p(\bar{\mathbf{a}}_{1:M})$ can be written as the factor model $p(\theta_{1:k}, \bar{\mathbf{x}}, \bar{\mathbf{z}}, \bar{\mathbf{a}})$ then we obtain *sequential ignorable treatment assignment*:

$$\mathbf{Y}(\bar{\mathbf{a}}) \perp (A_{t1}, \dots, A_{tk}) \mid \bar{\mathbf{X}}_t, \bar{\mathbf{Z}}_t, \bar{\mathbf{A}}_{t-1}, \quad (33)$$

for all $\bar{\mathbf{a}} \in \bar{\mathcal{A}}$ and for all $t \in \{0, \dots, T\}$.

Proof for Theorem 1:

Theorem 1 follows from Lemmas 1 and 2. In particular, using the proposed factor graph, we can obtain a sequential Kallenberg construction at each timestep and then obtain sequential ignorability.

B. Implementation details for the factor model

The factor model described in Section 5 was implemented in Tensorflow (Abadi et al., 2015). For each synthetic dataset (simulated as described in Section 6.1), we obtained 5000 patients, out of which 4000 were used for training, 500 for validation and 500 for testing. Using the validation set, we perform hyperparameter optimisation using 30 iterations of random search to find the optimal values for the learning rate, minibatch size (M), RNN hidden units, multitask FC hidden units and RNN dropout probability. LSTM (Hochreiter & Schmidhuber, 1997) units are used for the RNN implementation. The search range for each hyperparameter is described in Table 2.

The trajectories for the patients do not necessarily have to be equal. However, to be able to train the factor model, we zero padded them such that they all had the same length. The patient trajectories were then grouped into minibatches of size M and the factor model was trained using the Adam optimiser (?) for 100 epochs.

Table 2. Hyperparameter search range for the proposed factor model implemented using a recurrent neural network with multitask output and variational dropout.

Hyperparameter	Search range
Learning rate	0.01, 0.001, 0.0001
Minibatch size	64, 128, 256
RNN hidden units	32, 64, 128, 256
Multitask FC hidden units	32, 64, 128
RNN dropout probability	0.1, 0.2, 0.3, 0.4, 0.5

Table 3 illustrates the optimal hyperparameters obtained for the factor model under the different amounts of hidden confounding applied (as described by the experiments in Section 6.1). Since the results for assessing the Time Series Deconfounder are averaged across 30 different simulated datasets, we report here the optimal hyperparameters identified through majority voting. We note that when the effect of the hidden confounders on the treatment assignments and the outcome is large, more capacity is needed in the factor model to be able to infer them.

Table 3. Optimal hyperparameters for the factor model when different amounts of hidden confounding are applied in the synthetic dataset. The parameter γ measures the amount of hidden confounding applied.

Hyperparameter	$\gamma = 0$	$\gamma = 0.2$	$\gamma = 0.4$	$\gamma = 0.6$	$\gamma = 0.8$
Learning rate	0.01	0.01	0.01	0.01	0.001
Minibatch size	64	64	64	64	128
RNN hidden units	32	64	64	128	128
Multitask FC hidden units	64	128	64	128	128
RNN dropout probability	0.2	0.2	0.1	0.3	0.3

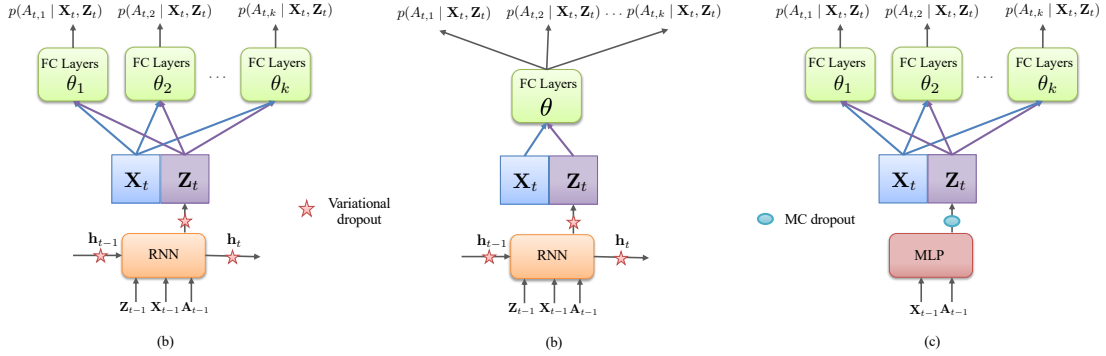


Figure 6. (a) Proposed factor model using recurrent neural network with multitask output and variational dropout. (b) Alternative design without multitask output. (c) Factor model using an MLP (shared across timestep) and multitask output. This baseline does not capture time-dependencies. MC dropout (Gal & Ghahramani, 2016a) is applied in the MLP to be able to sample from the substitute hidden confounders.

C. Baselines for evaluating factor model

Figure 6 illustrates the architecture at each timestep for our proposed factor model and for the baselines used for comparison. Figure 6(a) represents our proposed architecture for the factor model consisting of a recurrent neural network with multitask output and variational dropout. We want to ensure that the multitask constraint does not cause a decrease in the capability of the network to capture the distribution of the assigned causes. In order to do so, we compare our proposed factor model with the network in Figure 6(b) where we predict the k treatment assignments by passing X_t and Z_t through a hidden layer and having an output layer with k neurons. Moreover, to highlight the importance of learning time-dependencies in order to estimate the substitutes for the hidden confounders, we also use as a baseline the factor model in Figure 6(c). In this case, a multilayer perceptron (MLP) is shared across the timesteps and it infers the latent variable Z_t using only the previous covariates and treatments. Note that in this case there is no dependency on the entire history.

The baselines were optimised under the same set-up described for our proposed factor model in Appendix B. Tables 4 and 5 describe the search ranges used for the hyperparameters in each of the baselines.

Table 4. Hyperparameter search range for factor model without multitask (Figure 6(b)).

Hyperparameter	Search range
Learning rate	0.01, 0.001, 0.0001
Minibatch size	64, 128, 256
Max gradient norm	1.0, 2.0, 4.0
RNN hidden units	32, 64, 128, 256
Multitask FC hidden units	32, 64, 128
RNN dropout probability	0.1, 0.2, 0.3, 0.4, 0.5

Table 5. Hyperparameter search range for MLP factor model. Figure 6(c))

Hyperparameter	Search range
Learning rate	0.01, 0.001, 0.0001
Minibatch size	64, 128, 256
MLP hidden layer size	32, 64, 128, 256
Multitask FC hidden units	32, 64, 128
MLP dropout probability	0.1, 0.2, 0.3, 0.4, 0.5

D. Outcome models

After inferring the substitutes for the hidden confounders using the factor model, we implement outcome models to estimate the individualised treatment responses:

$$\mathbb{E}[\mathbf{Y}_{t+1} \mid \bar{\mathbf{A}}_t, \bar{\mathbf{X}}_t, \bar{\mathbf{Z}}_t] = h(\bar{\mathbf{A}}_t, \bar{\mathbf{X}}_t, \bar{\mathbf{Z}}_t) \quad (34)$$

Note that, by setting $t = T$ this is equivalent to the problem formulation in Section 3. However, in this case, we repeat the outcome problem, as formulated in Section 3 for each timestep in the sequence. Thus, we train the outcome models and evaluate them on predicting the treatment responses for each timestep, i.e. one-step-ahead predictions.

For training and tuning the outcome models, we use the same train/validation/test splits that we have used for the factor model. This means that the substitutes for the hidden confounders estimated using the fitted factor model on the test set are also used for testing purposes in the outcome models.

D.1. Marginal Structural Models

MSMs (Robins et al., 2000; Hernán et al., 2001) have been widely used in epidemiology to perform causal inference in longitudinal data. MSMs compute propensity weights to construct a pseudo-population from the observational data that resembles the one in a clinical trial and thus remove the selection bias and the bias introduced by time-dependent confounders (Platt et al., 2009). The propensity scores for each patient in the training set are computed as follows:

$$SW = \prod_{i=1}^t \frac{f(\mathbf{A}_t \mid \bar{\mathbf{A}}_{t-1})}{f(\mathbf{A}_t \mid \bar{\mathbf{X}}_t, \bar{\mathbf{Z}}_t, \bar{\mathbf{A}}_{t-1})} = \prod_{i=1}^t \frac{\prod_{j=1}^k f(A_{t,j} \mid \bar{\mathbf{A}}_{t-1})}{\prod_{j=1}^k f(A_{t,j} \mid \bar{\mathbf{X}}_t, \bar{\mathbf{Z}}_t, \bar{\mathbf{A}}_{t-1})} \quad (35)$$

where $f(\cdot)$ is the conditional probability mass function for discrete treatments and the conditional probability density function for continuous treatments.

We adopt the implementation in (Hernán et al., 2001; Howe et al., 2012) for MSMs and estimate the propensity weights using logistic regression as follows:

$$f(A_{t,k} \mid \bar{\mathbf{A}}_{t-1}) = \sigma\left(\sum_{j=1}^k \omega_k \left(\sum_{i=1}^{t-1} A_{t,j}\right)\right) \quad (36)$$

$$f(A_{t,k} \mid \bar{\mathbf{X}}_t, \bar{\mathbf{Z}}_t, \bar{\mathbf{A}}_{t-1}) = \sigma\left(\sum_{j=1}^k \phi_k \left(\sum_{i=1}^{t-1} A_{t,j}\right) + \mathbf{w}_1 \mathbf{X}_t + \mathbf{w}_2 \mathbf{X}_{t-1} + \mathbf{w}_3 \mathbf{Z}_t + \mathbf{w}_4 \mathbf{Z}_{t-1}\right) \quad (37)$$

where ω_* , ϕ_* and \mathbf{w}_* are regression coefficients and $\sigma(\cdot)$ is the sigmoid function.

For predicting the outcome, the following regression model is used, where each individual patient is weighted by its propensity score:

$$h(\bar{\mathbf{A}}_t, \bar{\mathbf{X}}_t, \bar{\mathbf{Z}}_t) = \sum_{j=1}^k \beta_k \left(\sum_{i=1}^t A_{t,j}\right) + \mathbf{l}_1 \mathbf{X}_t + \mathbf{l}_2 \mathbf{X}_{t-1} + \mathbf{l}_3 \mathbf{Z}_t + \mathbf{l}_4 \mathbf{Z}_{t-1} \quad (38)$$

where β_* and \mathbf{l}_* are regression coefficients. Since MSMs do not require hyperparameter tuning, we train them on the patients from both the train and validation sets.

D.2. Recurrent Marginal Structural Networks

R-MSNs, implemented as described in (Lim et al., 2018)², use recurrent neural networks to estimate the propensity scores and to build the outcome model. The use of RNNs is more robust to changes in the treatment assignment policy. Moreover, R-MSNs represent the first application of deep learning in predicting time-dependent effects. The propensity weights are estimated using recurrent neural networks as follows:

$$f(A_{t,k} \mid \bar{\mathbf{A}}_{t-1}) = \text{RNN}_1(\bar{\mathbf{A}}_{t-1}) \quad f(A_{t,k} \mid \bar{\mathbf{X}}_t, \bar{\mathbf{Z}}_t, \bar{\mathbf{A}}_{t-1}) = \text{RNN}_2(\bar{\mathbf{X}}_t, \bar{\mathbf{Z}}_t, \bar{\mathbf{A}}_{t-1}) \quad (39)$$

²We used the publicly available implementation from https://github.com/sjblim/rmsn_nips_2018.

For predicting the outcome, the following prediction network is used:

$$h(\bar{\mathbf{A}}_t, \bar{\mathbf{X}}_t, \bar{\mathbf{Z}}_t) = \text{RNN}_3(\bar{\mathbf{X}}_t, \bar{\mathbf{Z}}_t, \bar{\mathbf{A}}_t), \quad (40)$$

where in the loss function, each patient is weighted by its propensity score. Since the purpose of our method is not to improve predictions, but rather to assess how well the R-MSNs can be deconfounded using our method, we use the optimal hyperparameters for this model, as identified by (Lim et al., 2018). R-MSNs are then trained on the combined set of patients from the training and validation sets. Table 6 shows the hyperparameters used for training the R-MSNs.

Table 6. Hyperparameters used for R-MSNs.

Hyperparameter	Propensity networks		Prediction network
	$f(\mathbf{A}_t \bar{\mathbf{A}}_{t-1})$	$f(\mathbf{A}_t \bar{\mathbf{H}}_t)$	
Dropout rate	0.1	0.1	0.1
State size	6	16	16
Minibatch size	128	64	128
Learning rate	0.01	0.01	0.01
Max norm	2.0	1.0	0.5

R-MSNs (Lim et al., 2018), can also be used to forecast treatment responses for an arbitrary number of steps in the future. In our paper we focus on one-step ahead predictions of the treatment responses. However, the Time Series Deconfounder can also be applied for the long-term estimation of treatment effects.